Developmental Cell
Article

Aurora B and Cyclin B Have Opposite Effects on the Timing of Cytokinesis Abscission in *Drosophila* Germ Cells and in Vertebrate Somatic Cells

Juliette Mathieu,[1,2] Clothilde Cauvin,[6,8] Clara Moch,[1,2] Sarah J. Radford,[3] Paula Sampaio,[4] Carolina N. Perdigoto,[1,2,5,7] François Schweisguth,[5,7] Allison J. Bardin,[1,2,5,7] Claudio E. Sunkel,[4] Kim McKim,[3] Arnaud Echard,[6,8] and Jean-René Huynh[1,2,*]

[1]Department of Genetics and Developmental Biology, Institut Curie, F-75248 Paris, France
[2]UMR3215, Inserm U934, CNRS, F-75248 Paris, France
[3]Waksman Institute and Department of Genetics, Rutgers University, Piscataway, NJ 08854, USA
[4]IBMC - Instituto de Biologia Molecular e Celular, Universidade do Porto, 415-180 Porto, Portugal
[5]Developmental Biology Department
[6]Membrane Traffic and Cell Division G5 Laboratory
Institut Pasteur, F-75015 Paris, France
[7]URA2578
[8]URA2582
CNRS, F-75015 Paris, France
*Correspondence: jean-rene.huynh@curie.fr
http://dx.doi.org/10.1016/j.devcel.2013.07.005

SUMMARY

Abscission is the last step of cytokinesis that physically separates the cytoplasm of sister cells. As the final stage of cell division, abscission is poorly characterized during animal development. Here, we show that Aurora B and Survivin regulate the number of germ cells in each *Drosophila* egg chamber by inhibiting abscission during differentiation. This inhibition is mediated by an Aurora B-dependent phosphorylation of Cyclin B, as a phosphomimic form of Cyclin B rescues premature abscission caused by a loss of function of Aurora B. We show that Cyclin B localizes at the cytokinesis bridge, where it promotes abscission. We propose that mutual inhibitions between Aurora B and Cyclin B regulate the duration of abscission and thereby the number of sister cells in each cyst. Finally, we show that inhibitions of Aurora B and Cyclin-dependent kinase 1 activity in vertebrate cells also have opposite effects on the timing of abscission, suggesting a possible conservation of these mechanisms.

INTRODUCTION

During animal development, the canonical cell cycle is modulated and adapted in different cell types. How specific developmental programs alter different steps of the cell cycle remains to be understood in most cases. In this respect, the last stages of cell division, when daughter cells become separated, are probably the most diverse but also the least explored. In sea urchin embryos, the timing of cytokinesis is shifted and the completion of cell division only occurs during the S phase of the next cycle (Sanger et al., 1985). Cytokinesis altogether is absent during megakaryocyte differentiation and can also be arrested at a late stage in spermatocytes of most species (Pepling et al., 1999; Vitrat et al., 1998). Cytokinesis starts by the specification of a cleavage plane and is followed by the ingression of an actomyosin contractile ring. During this transition, the mitotic spindle rearranges at the midzone to form an electron-dense structure known as the midbody at the center of the intercellular bridge. Daughter cells then become physically separated by a process called abscission. It remains unclear what regulates the timing of abscission during animal development, which can vary from minutes to hours or can even stay incomplete, as in germ cells (Pepling et al., 1999).

The timing and order of the cell cycle is driven by oscillations in the activities of conserved cyclin-dependent kinases (Cdk). A high Cdk-1 activity, mostly driven by Cyclin B/Cdk-1 in higher eukaryotes, allows the cell to enter and perform mitosis (Malumbres and Barbacid, 2009). Rising levels of Cyclin B (CycB) and its translocation into the nucleus prepare cells to enter M phase (Gavet and Pines, 2010a, 2010b). CycB/Cdk-1 then becomes fully active when inhibitory phosphorylations by Wee1 and Myt1 are removed by Cdc25 phosphatase on Cdk-1-activating sites (Lindqvist et al., 2009). Exit from mitosis is then initiated by the degradation of Cyclin B in metaphase, when the spindle assembly checkpoint is satisfied (Clute and Pines, 1999; Sigrist et al., 1995; Sullivan and Morgan, 2007). Consequently, CycB/Cdk-1 activity remains low until the next G1 phase. However, it is unknown whether these low levels of CycB/Cdk-1 have any function after anaphase (Wurzenberger and Gerlich, 2011). The sharp changes in CycB/Cdk-1 activity are due to positive and negative feedback loops between Cdk-1 and the kinases/phosphatases mentioned above. Additional families of kinases, such as Polo (Plk) and Aurora, impinge on these loops to further regulate CycB/Cdk-1 activity and to order multiple events downstream of the core regulators (Lindqvist et al., 2009). Among those, Aurora B (AurB) is known to regulate chromosome orientation

and attachment to the mitotic spindle at metaphase. AurB is the active kinase of a biochemical complex, named the chromosomal passenger complex (CPC). This complex is highly conserved in many species and also contains the Survivin, Incenp, and Borealin subunits, which regulate AurB localization and kinase activity (Ruchaud et al., 2007). In contrast to Cdk-1, Polo and AurB are known to play later functions during cell division, as they translocate from centromeres to the spindle midzone to participate in the early steps of cytokinesis, such as the ingression of the furrow (Adams et al., 2001; Burkard et al., 2007; Gruneberg et al., 2004; Neef et al., 2003; Petronczki et al., 2007; Terada et al., 1998). The translocation of Aurora B to the midzone is, however, inhibited while CycB/Cdk-1 activity is still high at the metaphase-anaphase transition (Parry et al., 2003). Indeed, recent results showed that direct phosphorylation of the CPC by Cdk-1 targets Aurora B to the inner centromeres and prevents its localization to the spindle midzone through Mklp2 (Hümmer and Mayer, 2009; Tsukahara et al., 2010). At the midbody, Aurora B was shown recently to have an additional function near the very end of cytokinesis, during abscission. Studies in yeast and human cells demonstrated that Aurora B delays completion of cytokinesis until chromosomes are well separated after anaphase (Norden et al., 2006; Steigemann et al., 2009). This checkpoint, named the NoCut pathway, prevents lagging DNA to be cut by the cleavage furrow in order to avoid chromosome breakage. Aurora B thus has two different functions during cytokinesis, as it allows furrow ingression during the early steps but can also delay the completion of cytokinesis. It remains, however, unknown whether Aurora B also regulates abscission in vivo during normal animal development and if Aurora B acts at this stage with other mitotic kinases, such as Plks and Cdks.

Cytokinesis is blocked in germ cells of most species during at least some stage of their normal development (Pepling et al., 1999). A classic example is the *Drosophila* egg chamber, which is a syncytium of 16 cells produced by four rounds of mitosis of a single precursor, called a cystoblast (CB) (Huynh and St Johnston, 2004). Cystoblasts are produced throughout the life of adult females by germline stem cells (GSCs) located at the anterior tip of each ovary in the germarium (Figure 1A). Each stem cell self-renews by dividing asymmetrically to generate one stem cell, which stays in contact with support cells in the niche and receives signals that prevent differentiation (Chen et al., 2011). The second daughter cell is positioned outside of the niche, does not receive these signals, and thus starts to transcribe the *bam* gene, which is necessary and sufficient to trigger the transcription program of the cystoblast. This differentiation is characterized by four rounds of synchronous divisions, which form a 16-cell cyst made of 15 nurse cells and one oocyte. In the resulting cyst, each cytokinesis is arrested and all sister cells share the same cytoplasm through ring canals. In contrast, cytokinesis between the GSC and the CB is complete. It is, however, very slow, and GSCs and CBs remain synchronized until abscission is completed during the G2 phase of the next cycle, about 24 hr later (de Cuevas and Spradling, 1998). How abscission is regulated differently in GSCs and CBs is unknown. The orientation and synchrony of these divisions is controlled by a germline-specific organelle, called the fusome, which is made of endoplasmic reticulum (ER)-derived vesicles (Huynh, 2005). The fusome is partly inherited from the spectrosome of the GSCs (also made of ER-derived vesicles) and partly newly formed at the midbody during each division. Fusion between fusome precursors creates a continuum of vesicles going through each canal and connecting all the cells within a cyst (de Cuevas and Spradling, 1998; Snapp et al., 2004). Interestingly, cell cycle regulators, such as Cyclin A, Cyclin E, and subunits of the proteasome, localize on the fusome, which may help to synchronize their activation and destruction in all cells (Lilly et al., 2000; Lilly and Spradling, 1996; Ohlmeyer and Schüpbach, 2003). The pattern of divisions is invariant, with eight cells with one ring canal, four cells with two, two cells with three, and two cells with four. This pattern is important, as the oocyte always differentiates from one of the two cells with four ring canals, which are called the pro-oocytes (Spradling, 1993b). Incidentally, the number of ring canals in each cell can be used as a marker for the number of divisions (Figure 1A).

RESULTS

Loss-of-Function Mutations in *Aurora B* and *Survivin* Reduce the Number of Germ Cells per Egg Chamber

We identified two complementation groups of several alleles affecting the early steps of germ-cell development in *Drosophila* ovaries (see Supplemental Experimental Procedures available online for details). In hypomorphic conditions, mutant egg chambers were made of eight germ cells instead of 16, and the oocyte was linked to only three nurse cells by three ring canals instead of four (Figures 1B–1D). These results suggested that these mutant egg chambers had gone through three divisions instead of four. In strong loss-of-function conditions, induced using the FLP/FRT recombination target system, we observed the formation of giant GSCs filling the entire germarium (Figures S2A–S2C). These mutant cells had highly polyploid nuclei, enlarged spectrosomes, and did not come out of the germarium.

The first complementation group was made of three ethyl methanesulfonate (EMS)-induced alleles called 2A43, 35.33, and 1689. We genetically mapped these mutations to the *ial* (*Ipl1-aurora-like kinase*) locus, which encodes the *Drosophila* homolog of Aurora B (the locus is referred as *aurB* hereafter) (Figure 1F). 2A43 and 35.33 are the strongest alleles and both are homozygous lethal. They correspond to alterations in the most conserved part of the protein, with a leucine to phenylalanine substitution at position 166 (35.33) and a frame shift followed by a truncation in the kinase activation loop (2A43) (Figure 1F). In contrast, 1689 is a hypomorphic and viable allele, corresponding to a proline to serine substitution in the nonconserved N-terminal part of the protein (Figure 1F). The second complementation group is made of two PiggyBac insertions that we generated (PBac2180; Mathieu et al., 2007) or found in public stock collection (PBac{RB}e01527). Both transposons are inserted in the 5′ regulatory region of the *deterin* locus (also called dSurvivin), which encodes the *Drosophila* homolog of Survivin, referred as *svn* hereafter (Figure 1G; Jones et al., 2000). Both alleles produced very little *svn* RNA (data not shown) and were homozygous lethal at the pupal stage. We confirmed that all phenotypes were only due to the lack of *aurB* or *svn*, as wild-type genomic transgenes encoding *aurora B* or *svn* could rescue viability and mitotic phenotypes (Figures S1D and S1E). Aurora B and Survivin are known to be part of the highly conserved CPC, and as expected

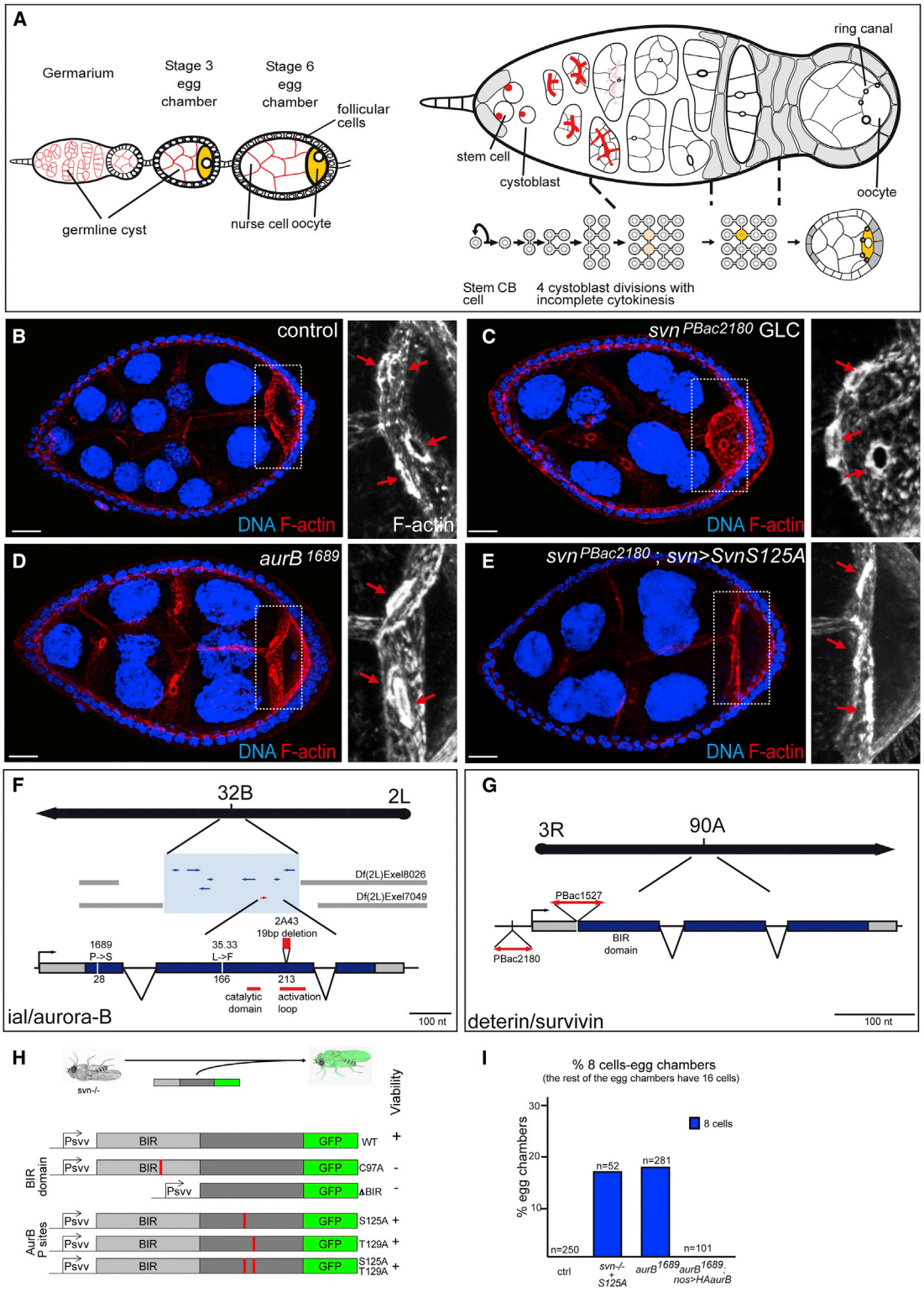

Figure 1. Identification of *Survivin* and *Aurora B* Loss-of-Function Alleles

(A) Scheme showing an ovariole with a germarium linked to two growing egg chambers (left), and a close-up on a germarium (right). The egg chambers are formed of 16 germline cells, 15 nurse cells, and one oocyte (in yellow), surrounded by a follicular epithelium. The egg chamber matures from germline stem cell to germline cyst (left to right) and encapsulation of the cyst by follicular cells in the germarium. At the anterior tip of the germarium, the germline stem cell divides asymmetrically and produces a cystoblast (CB). The spectrosome in the GSC and the fusome in its progeny (in red in the right scheme) are germline-specific organelles. Anterior is on the left, posterior on the right.

(legend continued on next page)

from the well-described roles of the CPC in mitosis, highly polyploid nuclei were not specific to mutant germ cells but were found in any dividing cell types, such as larval neural stem cells (Figures S2D, S2E, and S2F–S2M; Movies S1 and S2).

We took advantage of the absence of endogenous Svn in our strong loss-of-function mutants to perform a structure/function analysis. We generated wild-type and mutant GFP-tagged transgenes based on a genomic rescue construct containing the endogenous promoter and regulatory sequences, and we tested their ability to rescue viability, ploidy, and the number of germ cells per cyst (Figure 1H). We found that a wild-type form of Svn could rescue perfectly viability and diploidy. It also localized as expected at centromeres during prophase and prometaphase and at the midzone and intercellular bridge during later mitosis (Figures S1A–S1C). In contrast, variants of Svn with a defective BIR domain were not able to rescue viability (Figure 1H), consistent with previous studies in cell culture (Lens et al., 2006; Yue et al., 2008). It has been proposed that Survivin could be phosphorylated by Aurora B in vitro on T117 in human cells (Wheatley et al., 2004). We found two residues (S125 and T129) fitting the consensus of phosphorylation by Aurora B in *Drosophila* Survivin. However, they both appeared dispensable for fly viability. Indeed, nonphosphorylatable transgenes (SvnS125A and SvnT129A either mutated together or separately) rescued localization (not shown), viability, and diploidy to wild-type level (Figures 1H and S2N). However, they did not rescue the number of germ cells per egg chamber (Figures 1E and 1I). Both $svn^{-/-}$; *svn*>SvnS125A and $svn^{-/-}$; *svn*>SvnS125A,T129A females produced around 20% (17%; n = 52) of egg chambers with only eight cells, as we observed in hypomorphic $aurB^{1689}$ mutant flies (18%; n = 281; Figure 1I).The remaining cysts had 16 cells, as in wild-type condition. Furthermore, $svn^{-/-}$; *svn*>SvnWT females were perfectly rescued: 100% of cysts with 16 cells, n = 115. $svn^{-/-}$; *svn*>SvnS125A flies thus correspond to a weak loss-of-function condition. We concluded that our strong loss-of-function alleles of *aurB* and *svn* recapitulated the known functions of the CPC in a multicellular organism, while the weaker alleles revealed a developmental requirement of the CPC in the regulation of the number of germ cells per egg chamber.

Gain-of-Function Mutations in *Aurora B* and *Survivin* Increase the Number of Germ Cells per Egg Chamber

Next, we performed the converse experiment by overexpressing wild-type forms of Svn or AurB using the *nanos*-Gal4 driver (*nos*>), which is expressed specifically in all germ cells of the germarium (Figure 2E). We found that in these *nos*>Svn or *nos*>AurB females, a significant number of egg chambers had 32 cells and an oocyte with five ring canals, suggesting that they resulted from one extra division (Figures 2A, 2B, and 2G). As a control experiment, overexpression of Aurora A with the same driver did not induce any extra germ cell (Figure 2G). To mimic constitutive phosphorylation of Svn at the AurB consensus site, we overexpressed a SvnS125E form. We observed a dramatic increase in both the number of germ cells per cyst and the penetrance of the phenotype (Figures 2C and 2G). Almost 50% of *nos*>SvnS125E egg chambers had 32 cells or even more, as we found oocytes with six ring canals (Figures 2C and 2G). Furthermore, an insertion of SvnS125E expressed at a low level gave the same percentage of extra germ cells than a strongly expressed wild-type Svn, indicating that SvnS125E is more potent than Svn (Figures 2D and 2G). Importantly, the activity of SvnS125E still depended on the CPC, as removing one copy of the endogenous *svn*, *aurB*, or *Incenp* gene partially suppressed the extra germ cells phenotype (Figure S3A). These results indicated that SvnS125E fulfills the genetic definition of a hypermorphic allele of the CPC in our system. We thus concluded that loss of function of the CPC led to less germ cells per cyst, while gain of function of the CPC increased the number of germline cells per cyst.

We reasoned that if extra germ cells were caused by additional mitoses in the cyst, one would expect the phenotype to be autonomous to the cyst. We thus expressed SvnS125E only in dividing germline cysts using the *bam*-Gal4 driver (*bam*>), which is expressed from cystoblasts to eight cell cysts but not in GSCs (Figure 2F). To our surprise, we did not detect any extra germ cells (Figure 2G). Our results strongly suggested that it was the activity of SvnS125E in cells expressing *nanos* but not *bam* (i.e., mainly GSCs and some precystoblasts), which induced extra germ cells in the cyst.

Gain of Function of the CPC Leads to the Formation of Stem Cysts

How might stem cells regulate the number of divisions of their daughter cells? To address this question, we performed live imaging of GSCs expressing *nos*>SvnS125E-GFP. Surprisingly, these GSCs were dividing synchronously with several neighboring germ cells (Figure 3A; Movie S3; n = 9/10), suggesting that they may be physically connected, which is never seen in a wild-type situation (n > 50 in wild-type [WT]; Figure S7; Movie S7). We then analyzed the spectrosome in these GSCs and found that spectrosomes were branched as fusomes and linked GSCs with up to eight other germ cells (44.7%; n = 85; Figure 3B). These results pointed to an arrest of cytokinesis and showed that these cells were connected by a fusome, which could explain their synchrony in mitosis. To characterize whether these groups of cells were stem cells or cyst cells, we used several markers of identity. These clusters did not express Bam, a differentiation marker of the cyst (Figures 3C and 3D) but weakly expressed Nanos, like in stem cells (Figures 3E and 3F; Gilboa and Lehmann, 2004; McKearin and Ohlstein, 1995). Furthermore, only the cell in direct contact with niche cells was positive for p-Mad, a reporter of the Dpp pathway activation (Figures 3G and

(B–E) Stage 7 egg chambers from WT, $svn^{PBac2180}$ germline clone (GLC), ial^{1689}, or $svn^{PBac2180}$; *svn*>SvnS125A females stained with DAPI (DNA) and phalloidin (F-actin). On the right, close-up on oocytes. Red arrows indicate the four ring canals in the control oocyte and the three ring canals in the mutant backgrounds.
(F and G) Mapping of the *ial*/*aurB* and *deterin*/*svn* alleles.
(H) Structure of the *svn* transgenes generated and their ability to rescue the viability of the $svn^{PBac2180}$ mutants.
(I) Fraction of egg chambers exhibiting less than 16 cells (eight cells here) on the *y* axis. Genotypes are on the *x* axis.
Scale bar, 10 μm. See also Figures S1 and S2.

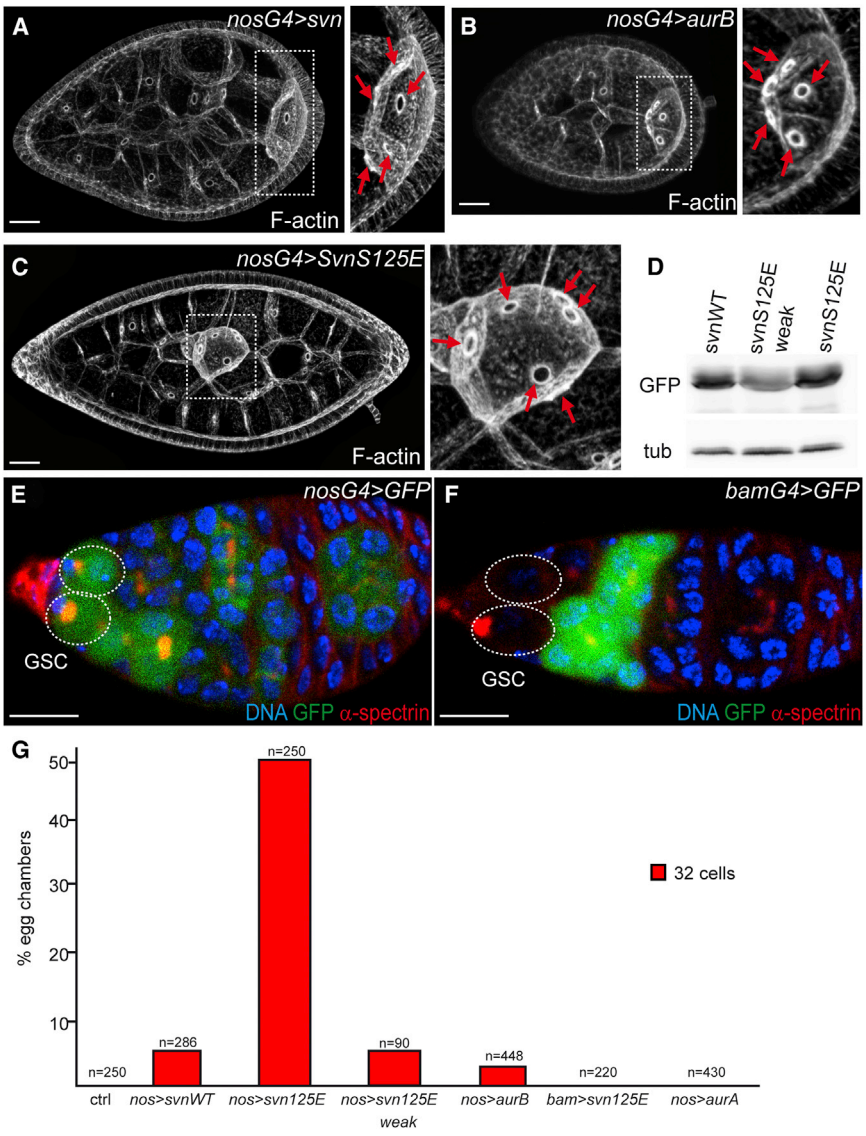

Figure 2. Svn and the CPC Regulate the Number of Germ Cells per Egg Chamber

(A–C) Stage 7 egg chambers of females expressing SvnWT-GFP (A), HA-AurB (B), or SvnS125E-GFP (C) under the control of the *nanos*-Gal4 driver (*nosG4*) stained with phalloidin. On the right, close-up on the oocyte. Red arrows indicate the five, five, and six oocyte ring canals in SvnWT-GFP (A), HA-AurB (B), or SvnS125E-GFP (C), respectively.

(D) Ovaries from females expressing Svn-GFP variants, WT or S125E, were processed for western blot analyses. Two insertions of SvnS125E-GFP (second and third lanes) are shown.

(E and F) Germaria of females expressing GFP under the control of the *nanos*-Gal4 (E, *nosG4*) and *bam*-Gal4 (F, *bamG4*) drivers stained with DAPI and α-spectrin. The GSCs (surrounded by dotted lines) are GFP positive with *nosG4*, not with *bamG4*.

(G) Fraction of egg chambers exhibiting more than 16 cells on the *y* axis. Genotypes are on the *x* axis. Scale bar, 10 μm. See also Figures S3 and S6.

The CPC Regulates Abscission in the Germline Stem Cell Lineage

The CPC is known to be required for furrow ingression during cytokinesis, but an excess of its activity later on at the midbody was recently proposed to delay abscission (Norden et al., 2006; Steigemann et al., 2009). In the germline, we noticed that Svn localized on the fusome, which forms at the midbody in both GSCs and differentiated cysts (Figure 5A). We further observed that SvnS125E localized like Svn on the fusome (Figure 4A). We reasoned that this concentration of SvnS125E at the fusome/midbody may cause the abscission delay in GSCs. To test this idea, we expressed *nos*>SvnS125E in *hts* mutant ovaries, which totally lack a fusome (Yue and Spradling, 1992), and counted the number of synchronous cells dividing, one being attached to the niche. On average, we found that three cells were dividing simultaneously in *nos*>SvnS125E stem cysts. In the absence of fusome, we mostly found single GSC dividing like in the wild-type control (Figures 4B–4E and S7; Movie S7). We thus concluded that the fusome played a key role in the formation of stem cysts and the inhibition of abscission by SvnS125E.

Overall, our results showed that the extra germ cells induced by a gain of function of the CPC are caused by an abscission delay in GSCs. We thus hypothesized that the reduction of germ cell number upon loss of function of the CPC may be caused by premature abscission in the cyst. In this model, complete abscission of a two-cell cyst will give rise to two single cells carrying on to make the three remaining divisions, thus generating two cysts of eight cells (Figure 4M). In support of this model, we observed in hypomorphic *aurB*^{1689} mutants two-cell 3H; Song et al., 2004). These synchronous cells thus had characteristics of both stem cells and cyst cells; we thus named them "stem cysts." Stem cysts may also represent an intermediate state of differentiation, as postulated previously (Gilboa et al., 2003).

These stem cysts did not grow indefinitely, however, and we observed that their fusome eventually broke down (Figures 3I and 3J, arrow), indicating that SvnS125E delayed abscission but did not block it completely. We thus hypothesized that complete abscission of the oldest links in stem cysts will generate "cystoblast-like" precursors made of two or more cells. In this model, a two-cell cystoblast will go through the regular four mitoses and give rise to a 32-cell cyst indistinguishable from a 32-cell cyst generated by five rounds of division of a single-cell precursor (Figures 3K and 3L). We thus proposed that 32-cell cysts did not come from extra mitoses in the cyst but that they could be generated by an abscission delay in GSCs and the formation of two-cell cystoblasts.

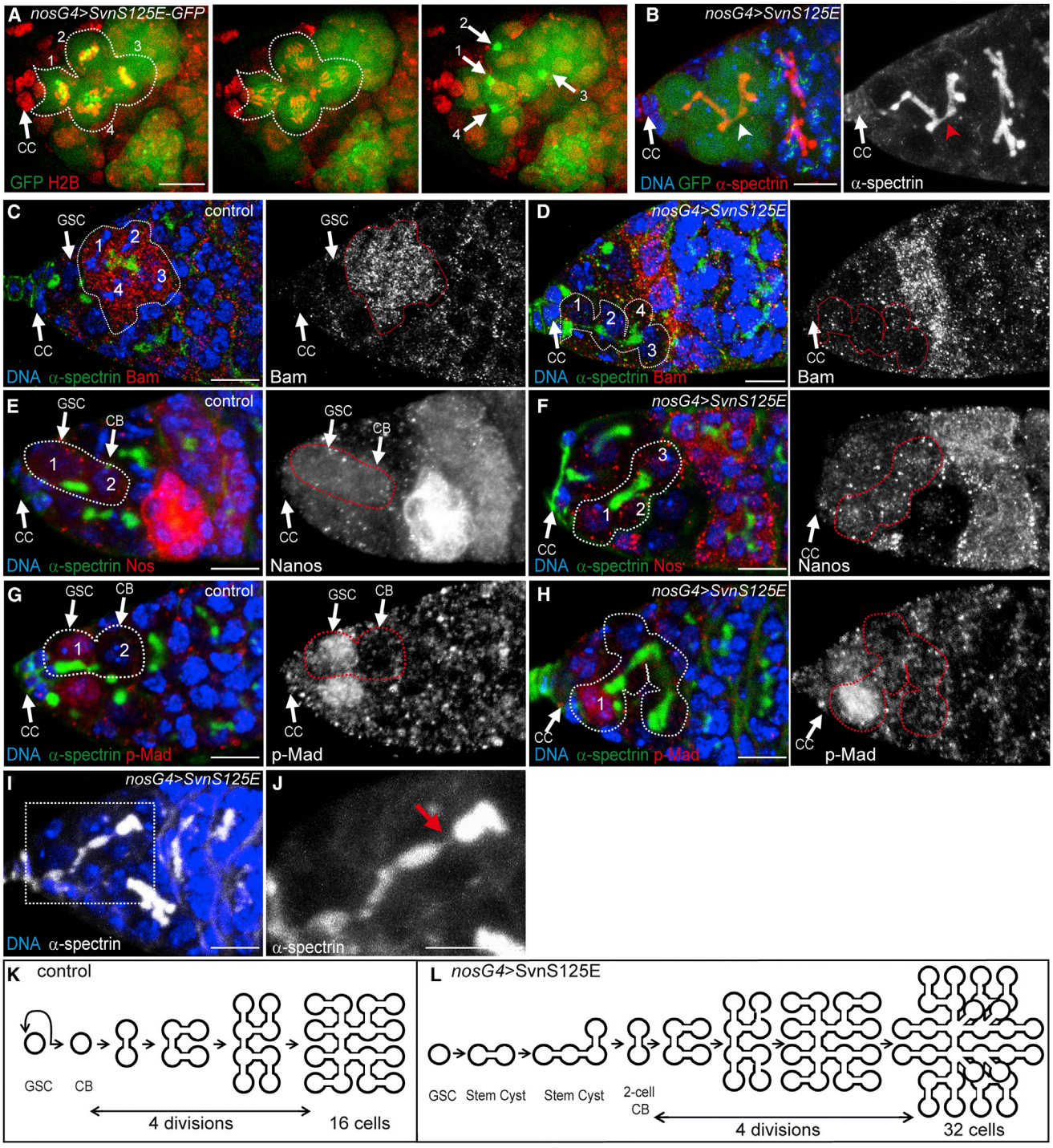

Figure 3. SvnS125E Generates Stem Cysts

(A) H2B-RFP in red, and SvnS125E-GFP in green. One GSC (attached to the cap cells) and three neighboring cells undergo mitosis synchronously.

(B) Expression of SvnS125E-GFP with *nanos*-Gal4 induces the formation of branched fusome (α-spectrin, red) in GSC attached to cap cell (CC).

(C–H) Germaria of WT females (C, E, and G) or females expressing SvnS125E under the control of *nanos*-Gal4 driver (*nosG4*), stained for α-spectrin (green), and either Bag of marble (Bam, C and D, red), Nanos (E and F, red), or p-Mad (G and H, red).

(I and J) Germarium expressing *nos*>SvnS125E. A branched fusome (white) is breaking at the posterior part (close-up in J). The red arrow indicates a thin thread of α-spectrin, probably the breaking point.

(K and L) Schemes representing the mitotic events in WT (K) and in SvnS125E (L) expressing germaria.

Scale bar, 10 μm. See also Figure S7 and Movies S3 and S7.

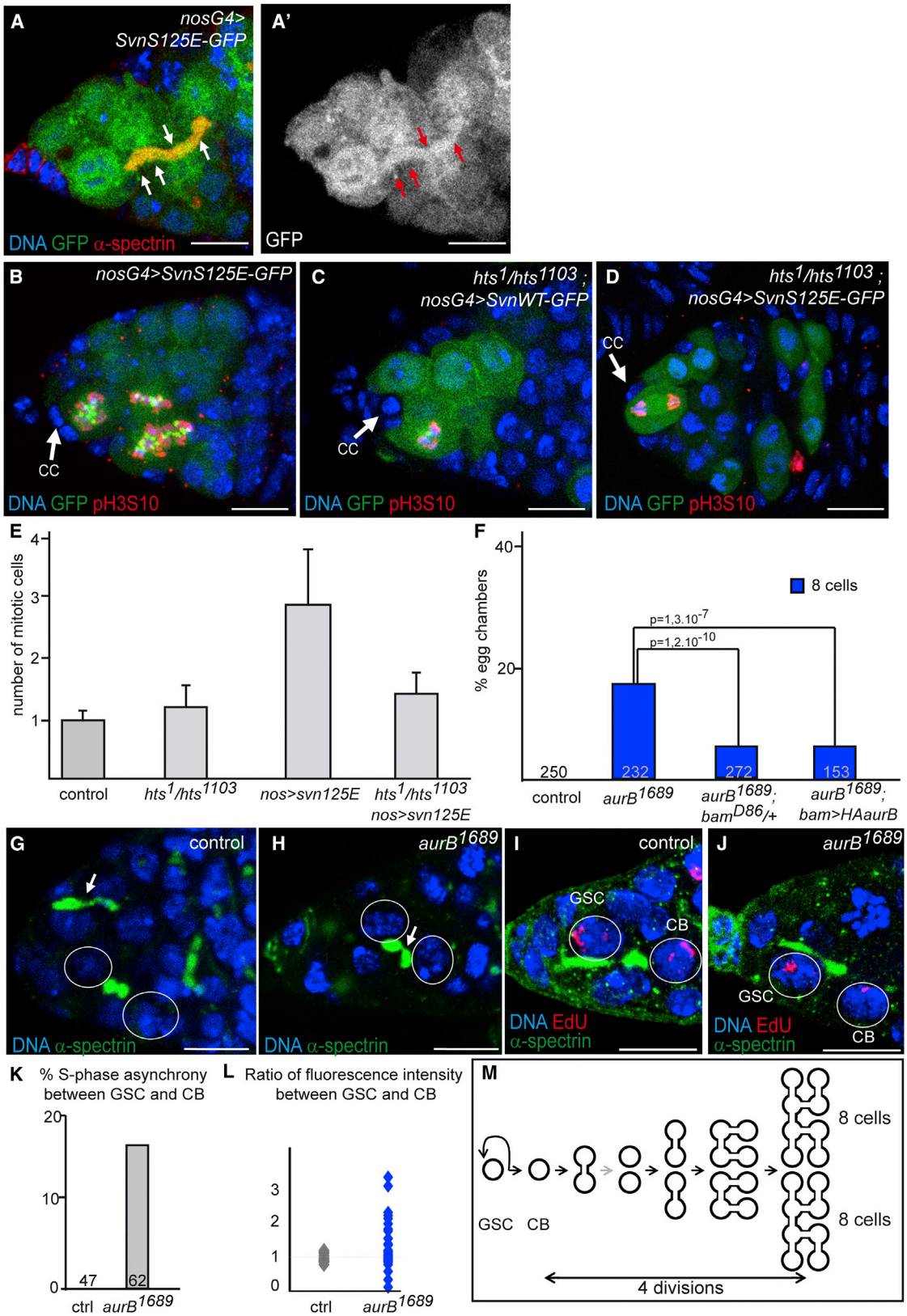

(legend on next page)

cysts linked by a thin thread of fusome, which indicates that abscission is about to be completed (Figures 4G and 4H, arrow). These threads of fusome are never seen in wild-type cysts but have been described during dedifferentiation experiments when cysts complete abscission and break into single cells (Kai and Spradling, 2004). We further noticed that eight cell cysts were found in pairs at a frequency three times higher than expected, if their distribution was random (0.048 observed versus 0.016 expected $p < 0.005$; see Supplemental Experimental Procedures), suggesting that each pair of eight cell cysts was derived from a single precursor. In addition, we found that removing one copy of *bam* strongly rescued *aurB*^{1689} phenotype (from 17% to 4% of eight cell cysts), indicating that the phenotype is caused by the reduction of AurB activity in the cyst and not in the GSC (Figure 4F). To validate this conclusion, we expressed a wild-type AurB transgene driven by the *bam* promoter in an *aurB*^{1689} homozygous background and found a strong rescue of the eight cell cyst phenotype (4%; n = 153; Figure 4F). Altogether, our results demonstrate that the CPC is required in the wild-type cyst to inhibit abscission during the first mitosis of the cystoblast (i.e., at the two-cell stage) and that abscission becomes precocious in *aurB*^{1689} mutant cysts. We further tested this conclusion in GSCs, which are known to remain connected and synchronous with their daughter CB until at least the G2 phase of the next cycle (de Cuevas and Spradling, 1998). Indeed, a 30 min pulse of ethynyl-deoxyuridine (EdU) equally labels GSC and CB, indicating that they replicated their DNA at the same time and thus that they were still connected during S phase of the following cycle. As reported previously, we found that all pairs of wild-type GSC and CB showed equal staining of EdU (100%; n = 47; Figures 4I, 4K, and 4L; de Cuevas and Spradling, 1998). In contrast, we found that GSC and CB were asymmetrically stained in 17% of *aurB*^{1689} mutant pairs (Figures 4J–4L; n = 62), revealing asynchronous behaviors already before or during S phase and suggesting complete abscission. We concluded that a reduction in Aurora B activity induced a precocious abscission in both GSCs and germline cysts.

Aurora B Is Required for Cyclin B Phosphorylation

Next, we asked what the targets of Aurora B that regulate the timing of abscission might be. To find putative substrates, we performed immunoprecipitations of Svn-GFP, AurB-red fluorescent protein (RFP), and hemagglutinin (HA)-AurB from embryos and sequenced the interactors by mass-spectrometry. We repeatedly found peptides matching CycB sequence, which caught our attention, as CycB was previously shown to regulate cell number of germline cysts (Lilly et al., 2000). We confirmed this interaction by coimmunoprecipitation of HA-Aurora B with Cyclin B-GFP (Figure 5C). We generated a full-length CycB-GFP transgene, which could rescue *cycB*-null mutant flies, and found that it localized like Svn on the GSC spectrosome and cyst fusome during interphase (red arrow on GSC1, Figure 5B). We analyzed its dynamic localization during mitosis and observed that it marked the centrosomes and kinetochores as expected (green arrows for the centrosomes, Figure 5B). Interestingly, we noticed that a pool of CycB-GFP accumulated at the intercellular bridge during late cytokinesis (red arrow, Figure 5D). A similar localization was found for endogenous CycB (Figure 5E). Reducing the level of CycB greatly enhanced *nos*>SvnS125E gain-of-function phenotype, demonstrating a negative genetic interaction between the CPC and CycB (Figure 5F). We also noticed five sites fitting the phosphorylation consensus of Aurora B in the N-terminal part of CycB. Two consensus sites are also present in the N-terminal region of human CycB2 (Figure 5G). In order to examine whether *Drosophila* Cyclin B was phosphorylated in vivo, we generated an antibody against a phosphopeptide corresponding to one of these sites (pS157) (Figure 5G). This antibody recognized CycB from wild-type extracts but not a nonphosphorylatable CycB-5A form, where all five sites were changed into alanines (Figure 5H). The alanine substitutions, however, may not be recognized by our antibody. To further test the specificity of our antibody, we treated wild-type ovarian extracts with lambda phosphastase. We found that, after this treatment, the wild-type form of Cyclin B was not recognized anymore by our anti-pCycB (Figure 5I), indicating that this antibody marked the phosphorylated form of CycB but not the unphosphorylated CycB (at least at S157). This result further demonstrated that the phosphorylated form of CycB at S157 existed in vivo in ovarian extracts. We next tested whether this phosphorylation event was dependent on Aurora B activity. We inhibited Aurora B with the widely used ZM447439 drug. We found a strong reduction of almost 50% in the pS157-CycB signal for equal amounts of total CycB (Figure 5J). We concluded that this phosphorylation depended on Aurora B activity. Taken together, our results demonstrate that AurB and CycB interact in vivo, that they both localize at the fusome and the midbody in the germline, and that phosphorylation of CycB at S157 depends on AurB activity.

Figure 4. The CPC Regulates Abscission in the Germline

(A) Germarium expressing *nos*>SvnS125E. SvnS125E-GFP (green and white in A′) colocalizes with α-spectrin (red) on the fusome (arrows).

(B–D) Germaria expressing either *nos*>SvnS125E-GFP (C and E) or *nos*>SvnWT-GFP (D) in a WT (C) or *hts* mutant background (D and E) stained with pH3S10 (red) to highlight mitotic cells.

(E) Number of synchronously dividing cells, counted only when the most anterior is a GSC. Error bars are SD.

(F) Fraction of egg chambers exhibiting less than 16 cells on the *y* axis. Genotypes are on the *x* axis. The penetrance of *aurB*^{1689} phenotype is rescued by a reduction in Bam level or by addition of AurB in the cyst only (bam>AurB).

(G and H) Germaria of WT (H) and *aurB*^{1689} (I) females stained for α-spectrin (green) and DNA (blue). (G) A snowman shape fusome observed in a two cell cyst. Abscission is occurring between a GSC and its daughter CB (arrow). (H) Breaking fusome in a *aurB*^{1689} mutant two cell cyst. Arrows point to a thin thread of fusome.

(I and J) Germaria of a WT (J) and an *aurB*^{1689} (K) female stained for EdU (red) and α-spectrin (green), showing S-phase synchrony between the GSC and its daughter CB in WT (J) but not in *aurB*^{1689} (K) females.

(K) Fraction of GSC/CB pair showing S-phase asynchrony on the *y* axis in %. Genotypes are on the *x* axis.

(L) GSC/CB ratios of EdU fluorescence in WT (gray) and in *aurB*^{1689} mutant (blue). S-phase synchrony is revealed by a ratio close to one.

(M) Scheme representing the mitotic events and premature abscission in *aurB*^{1689} germaria.

Scale bar, 10 μm. Error bars are SD. See also Figure S7 and Movie S7.

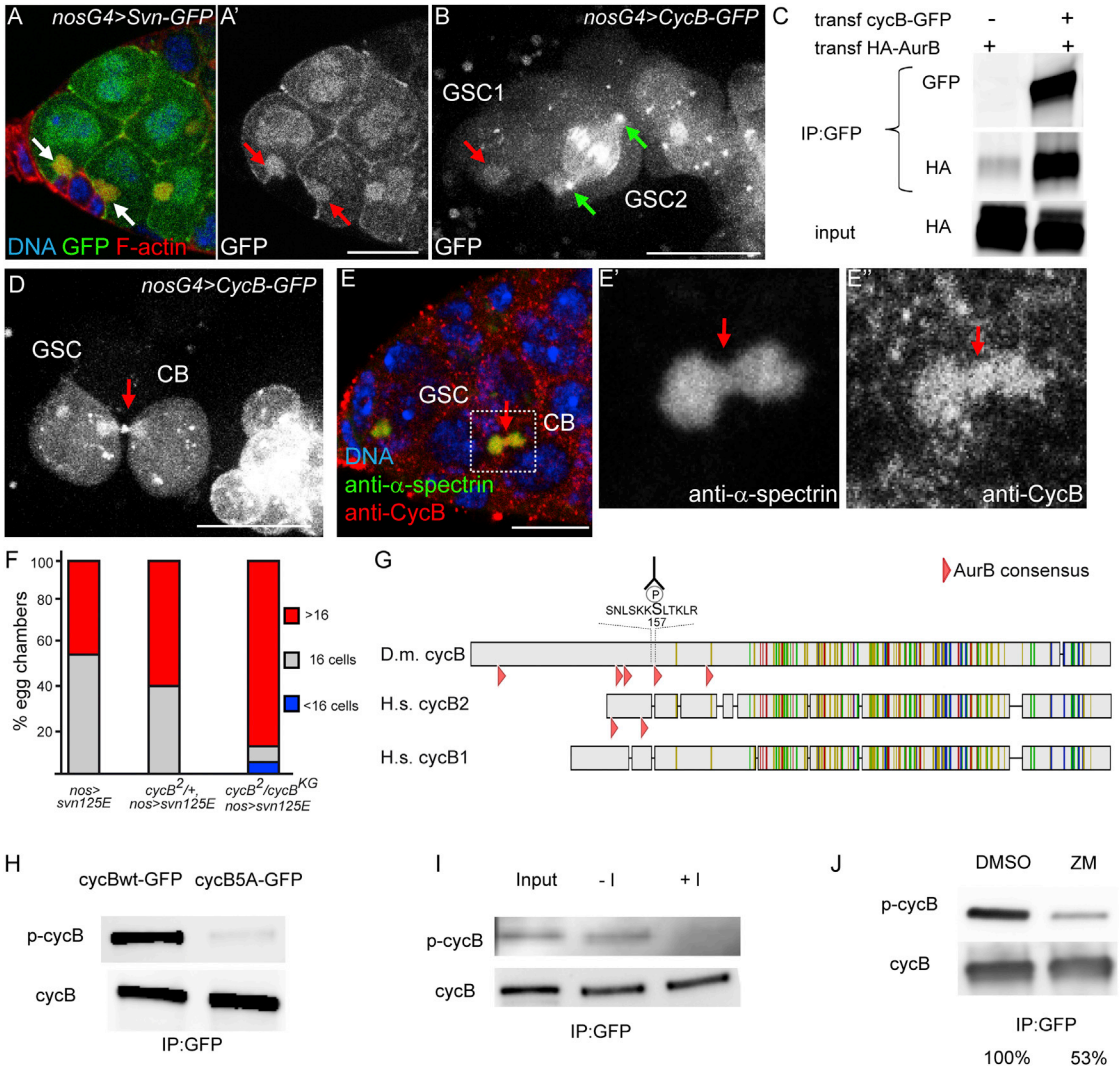

Figure 5. Aurora B Is Required for Phosphorylation of Cyclin B during Mitosis

(A) Germarium expressing *nos*>SvnWT-GFP stained with phalloidin (red) and DAPI (blue). GFP is in green. The spectrosome (arrows white in A, red in A′) is enriched in F-actin and SvnWT-GFP.

(B) Germarium expressing *nos*>CycB-WT-GFP, which localizes on the spectrosome (red arrow in GSC1) and centrosomes in metaphase (green arrows in GSC2).

(C) HEK293T cells were transfected with HA-AurB alone or with cycB-WT-GFP-expressing vectors and were processed for immunoprecipitation (IP) with anti-GFP antibody and western blot analyses with the GFP and HA antibodies. HA-AurB and CycB-GFP coimmunoprecipitate.

(D) Germarium expressing *nos*>CycB-WT-GFP. Note the presence of GFP at the midbody, linking the GSC and its CB (red arrow).

(E) Germarium of a WT female stained with anti-α-spectrin (green in overlay) and anti-Cyclin B (red in overlay) antibodies. Endogenous CycB localizes on the fusome and at the midbody (red arrows in E′ and E″).

(F) Fraction of egg chambers exhibiting less than 16 cells (blue), 16 cells (gray), and more than 16 cells (red) on the *y* axis. Genotypes are on the *x* axis. The penetrance of the SvnS125E phenotype (more than 16 cells) is enhanced by a reduction in CycB level.

(G) Alignment of *Drosophila melanogaster* Cyclin B with human Cyclin B1 and Cyclin B2. The pink arrowheads indicate Aurora B consensus site of the N-terminal regions of the different cyclins. The sequence of the phosphopeptide used to generate the phosphospecific Cyclin B antibody is shown (the p-serine is indicated by P).

(H) Embryos expressing CycB-WT-GFP or CycB-5E-GFP were processed for IP and western blot analyses with the p-CycB antibody or total CycB. CycB-5A is poorly recognized by the anti-p-CycB antibody.

(I) Embryos expressing CycB-WT-GFP were processed for IP and λ-phosphatase treatment followed by western blot analyses with the p-CycB antibody or total CycB. Upon λ-phosphatase treatment, the p-CycB positive band is not detected anymore.

(J) HEK293T cells transfected with CycB-WT-GFP expression vector were treated with ZM447439 or DMSO as a control, processed for IP, and analyzed by western blot, with anti-p-CycB antibody or anti-CycB. p-CycB level is diminished upon ZM447439 treatment. The percentages represent the amount of p-cycB detected relative to the one in DMSO-treated cells.

Scale bar, 10 μm. See also Figure S5.

Cyclin B Phosphorylation Regulates Abscission in the Germline Stem Cell Lineage

In order to test in vivo the potential role of the AurB-dependent phosphorylation of Cyclin B, we generated transgenic flies expressing a phosphomimic form of CycB at all five sites (CycB-5E). We found that *nos*>CycB-5E phenocopied *nos*>SvnS125E flies with a high percentage of 32-cell cysts containing an oocyte with five ring canals (Figures 6A and 6B). These 32-cell cysts were also generated by the formation of stem cysts rather than a fifth division, as we found branched fusomes originating from GSC in 55% of germaria (n = 47; Figure 6C) and synchronous divisions in stem cells expressing CycB-5E (Figure 6D; Movie S4), while these cells remained Bam negative (Figure 6E). In addition, we coexpressed a photoactivatable-GFP fused to α-tubulin, which could freely diffuse in the cytoplasm. We found that photoactivation with a two-photon laser of any cell of a stem cyst in G1/S phase (CycB-5E-GFP is absent in G1/S) led to a rapid diffusion of the fluorescence throughout the stem cyst, including the most anterior stem cell, which had not been activated (Figure 6F; Movies S5 and S6). We concluded that these cells were sharing the same cytoplasm and that abscission was incomplete in *nos*>CycB-5E stem cysts. Furthermore, expression of CycB-5E only in the cyst (*bam*>CycB-5E) had a wild-type phenotype, as observed when SvnS125E is also driven by *bam* (Figure 6B). In contrast, wild-type CycB or nonphosphorylatable CycB-5A induced a significant number of 32-cell cysts when expressed in the cyst (driven by the *bam* promoter) but not driven by the *nanos* promoter, indicating instead a fifth division in the cyst (Figure 6B).

CycB-5E delays abscission as a gain of function of the CPC, which we showed to negatively interact with CycB (Figure 5F). CycB-5E thus behaved as a dominant-negative form for Cdk-1 activity, at least regarding abscission. In support, coexpression of a wild-type CycB but not of a neutral GFP partially rescued the number of 32-cell cysts induced by CycB-5E (Figure 6G). If CycB-5E behaved as a dominant negative form, then one should expect the same phenotype in CycB loss of function. In the complete absence of CycB, mutant flies are viable but sterile, with almost no germ cells, as there is a specific requirement for CycB in germline stem cells self-renewal (Wang and Lin, 2005). To circumvent this problem, we expressed a newly developed RNA interference (RNAi) transgenic RNAi project (TRIP) line against CycB in GSCs, and we occasionally found stem cysts with branched fusomes (6.25%; n = 127) and resulting egg chambers made of 32 cells (13%; n = 44), as well as the expected eight-cell cysts (Figures 6H and 6I; Ni et al., 2011). These results are in agreement with CycB-5E being a dominant negative form. Nevertheless, CycB-5E could rescue *cycB* mutants' sterility (data not shown) and cycled like wild-type CycB (Movie S4; Figure S4).

Overall, our results showed that CycB promotes abscission and that its phosphorylation by Aurora B inhibits this activity. If Cyclin B was the main target of Aurora B during this process, one could make at least two predictions: (1) expression of the nonphosphorylatable CycB-5A should mimic the absence of AurB/Svn and (2) expression of phosphomimic CycB-5E should compensate for the absence of AurB/Svn. We found that the expression of CycB-5A induced the appearance of breaking fusome in two-cell cysts, as seen in $aurB^{1689}$mutant cysts (Figure 6J). We also detected asynchronous pairs of GSC/CB (16%; n = 26) similar to $aurB^{1689}$mutant pairs (17%; n = 62; Figures 6K and 6L). We concluded that, like in *aurB* mutants, abscission is precocious in GSC and two-cell cysts expressing CycB-5A. To test the second prediction, we expressed CycB-5E in $aurB^{1689}$ mutant cysts, in which we had found a premature abscission at the two-cell cyst stage (leading to the formation of eight-cell cysts). We found a strong reduction in the number of eight-cell cysts when $aurB^{1689}$ flies also expressed *bam*>-CycB-5E (from 14.5% to 3.5% of eight-cell cysts; Figures 6M and 6N). Importantly, this rescue was not the consequence of a combination of two phenotypes (32-cell cyst induced by CycB-5E, broken into two 16-cell cysts by $aurB^{1689}$ mutation), as we expressed CycB-5E with the *bam* promoter (i.e., only in the cyst and not in GSCs) and *bam*>CycB-5E had no phenotype on its own (Figure 6B). In contrast, *bam*>CycB and *bam*>CycB-5A induced a significant number of cysts with 32 cells, indicating that these forms were able to force an extra division in cysts (Figure 6B) and could not be used in an $aurB^{1689}$ mutant background. We thus concluded that loss of phosphorylation of CycB accounted for most phenotypes observed in $aurB^{1689}$ mutants and that CycB is a major target of the CPC in the regulation of abscission. Overall, our results showed that Aurora B delays abscission by antagonizing Cyclin B activity in *Drosophila* germ cells.

Cyclin B2 Localizes at the Intercellular Bridge, and Aurora B and Cdk-1 Have Opposite Effects on Abscission Timing in Human Cell Culture

As mentioned previously, Cyclin B2 in vertebrates, but not Cyclin B1, exhibits two consensus sites for Aurora B in its N-terminal domain (Figure 5G). We found that, in mouse embryonic fibroblasts (MEF), endogenous CycB2 localized at the intercellular bridge, where microtubules are less dense (Figure 7A). This signal was specific, as MEF derived from CycB2 knockout mice did not show this staining (Figure 7B). Human CycB2 tagged with GFP also localized at the intercellular bridge in HeLa cells (Figures 7C–7E). Next, we tested directly whether CycB2/Cdk-1 was required for abscission by inhibiting Cdk-1 activity only after the ingression of the cytokinetic furrow of HeLa cells. Drugs used to inhibit Cdk-1 (Cdk inhibitor III and RO-3306 [Gavet and Pines, 2010b]) were added well after metaphase (around 60 min; i.e., well after any known function of Cdk-1; Figure 7F). We found that both drugs induced a strong delay in the completion of abscission (Figure 7G; data not shown for RO-3306). Abscission duration was increased by 50% on average (216 min in control versus 317 min in treated cells p = 0.0056; Figure 7H). We concluded that Cdk-1 activity promotes abscission during late cytokinesis. Conversely, inhibition of Aurora B with the ZM447439 drug had the opposite effect and induced precocious abscission (171 min; Figure 7G), as previously reported (Steigemann et al., 2009). Furthermore, we found that the simultaneous inhibition of Aurora B and Cdk-1 restored normal timing (216 min in control versus 235 min in treated cells p = 0.135 [not significant]; Figures 7G and 7H). We concluded that Aurora B and Cdk-1 have opposite activities on abscission timing in mammalian cells.

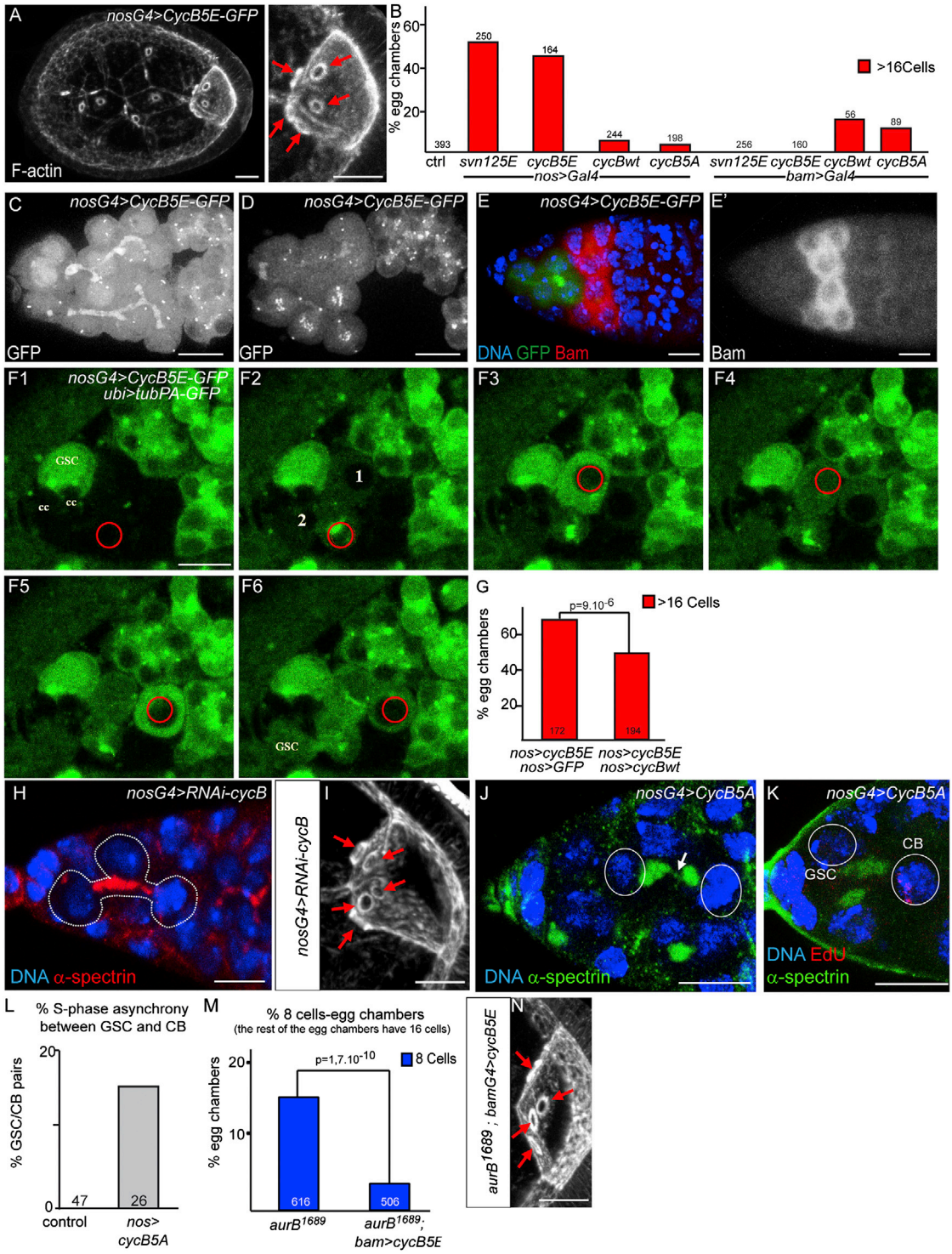

Figure 6. Cyclin B Phosphorylation Regulates Abscission in the Germline

(A) Stage 7 egg chambers expressing *nos*>CycB5E-GFP stained with phalloidin (F-actin). Red arrows indicate the five ring canals of the oocyte.

(B) Fraction of egg chambers exhibiting more than 16 cells on the *y* axis. Genotypes are on the *x* axis. CycB5E phenocopies SvnS125E.

(C and D) *nos*>CycB-5E-GFP localizes on the fusome in interphase. Stem cysts with branched fusomes form (C), and mitosis is synchronous within the stem cyst (D). In (D), four metaphase cells are visible, with GFP accumulation at the centrosomes, centromeres, and weakly on the fusome.

(E) Germarium expressing *nos*>CycB5E-GFP stained with DAPI (blue) and Bam (red, and white in E′). The stem cyst does not express Bam.

(F) Selected time points of a germarium expressing *nos*>CycB5E-GFP and *nos*>tubulin-PA-GFP. In F1, no CycB5E-GFP is visible in the selected cyst, because cells are in G1 or S phase. In F2, Tub-PA-GFP is photoactivated in a region defined by a red circle, and the fluorescence diffuses to cell 1 and cell 2 very rapidly. In

(legend continued on next page)

DISCUSSION

Aurora B and Cyclin B Regulate Abscission

Collectively, our data point to a simple model for the regulation of abscission in the germline. We propose that the accumulation of Aurora B on the fusome at the site of abscission creates a local activity of the CPC, which phosphorylates Cyclin B and delays abscission. In support of this model, we found that increasing the level and activity of the CPC delayed abscission in GSCs, while a decrease led to premature abscission in two-cell cysts. Conversely, a decrease in Cyclin B slowed down abscission in GSCs and counteracted premature abscission in mutant cysts with reduced Aurora B level (Figure 7I). Furthermore, inhibition of Cdk-1 after furrow ingression in HeLa cells delayed abscission, while inhibition of Aurora B led to faster abscission (Figures 7G and 7H). Our work also demonstrates that phosphorylation of CycB depends on Aurora B and inhibits CycB activity during late cytokinesis. Interestingly, this antagonistic relationship is reversed during early cytokinesis (Figure 7I), as high CycB/Cdk-1 blocks the initiation of cytokinesis (Echard and O'Farrell, 2003; Sigrist et al., 1995), while Aurora B is known to promote it (Ruchaud et al., 2007). Furthermore, it was recently shown that CycB/Cdk-1 can directly phosphorylate the CPC to trigger its localization to inner centromeres and inhibit its localization to the spindle midzone through Mklp2 (Gruneberg et al., 2004; Hümmer and Mayer, 2009; Tsukahara et al., 2010). On the one hand, CycB/Cdk-1 negatively regulates the localization of the CPC to the midzone and Aurora B function in the early steps of cytokinesis, and on the other hand, we found that the CPC negatively regulates CycB to inhibit abscission. We propose that a balance between the CPC and CycB/Cdk-1 mutual inhibition by phosphorylation plays a central role in the regulation of cytokinesis and abscission (Figure 7I).

How could this balance be shifted from complete cytokinesis in GSCs to arrest of abscission in differentiating cysts? One hypothesis is based on the difference of duration of the cell cycle between GSCs and germline cysts. GSCs enter mitosis and finish abscission every 24 hr. In contrast, differentiating cysts cycle much faster and undergo four cell cycles also in 24 hr (Morris and Spradling, 2011; Spradling, 1993a). Aurora B could delay abscission equally in GSCs and cystoblasts; however, GSCs would have the time to complete abscission, while cystoblasts would have already completed their four mitoses and differentiation program. Consistent with this hypothesis, when cyst differentiation is blocked at the two-cell stage in *bam* mutant ovaries, pairs of cells can be seen connected only by a thin thread of breaking fusome (McKearin and Ohlstein, 1995), similar to those we observed in $aurB^{1689}$ mutant cysts. In the absence of Bam, mutant ovaries accumulate single cells and pairs of cells, which are unable to differentiate and are delayed in that state (McKearin and Ohlstein, 1995). We thus propose that Aurora B delays abscission in wild-type GSCs and cystoblasts, and we speculate that cytokinesis can be completed, even in cystoblasts, if abscission becomes faster, such as in $aurB^{1689}$ mutants, or if differentiation is slower or arrested, such as in *bam* mutants.

Cyclin B Localization and Function at the Midbody

One surprising finding of our study is the presence and function of CycB at the end of cell division, which contrasts with the widely accepted view that all CycB is degraded during anaphase (Pines, 2006). Our live-imaging data showed that most of the wild-type and phosphomimic forms of CycB were indeed degraded at anaphase onset. However, a small pool of both forms accumulated later on at midbodies and at ring canals in differentiating cysts (Figures 5D, 5E, and S4B). This localization of CycB is conserved in several species, as we report that CycB2 also accumulates at the midbody in mouse and human cells (Figures 7A–7D). Interestingly, Clb2, a CycB homolog in yeast, was shown to localize at the bud neck (Eluère et al., 2007). Finally, Cdk-1 was also isolated from biochemically purified midbodies in a proteomic screen for functional components of cytokinesis (Skop et al., 2004). CycB and Cdk-1 thus localize at the midbody in several model systems.

Our genetic analysis showed that CycB plays an important function in counteracting Aurora B inhibition of abscission. This function may help to solve a lasting paradox of the regulation of the cell cycle in germ cells. Indeed, overexpression of string/cdc25, an activator of Cdk-1 that should force extra mitoses, instead induces mostly eight-cell cysts (Mata et al., 2000). Even more puzzling, a few 32-cell cysts are also produced in the same experiment. In contrast, overexpression of Tribbles (and Wee1 and Myt1 [Jin et al., 2005; S. Campbell, personal communication]), which are known inhibitors of Cdc25 and Cdk-1, produce 32 cell cysts rather than the expected eight-cell cysts (Mata et al., 2000). In agreement with these counterintuitive results, we found that reducing CycB levels could also produce some 32-cell cysts (Figure 6I). However, in light of our model, activation of Cdk-1 could lead to premature abscission

F3, PA-GFP is activated in cell 1 and in cell 3 in F5. In F6, all cells have the same level of fluorescence, including the GSC, which has not been directly activated. It demonstrates that Tub-PA-GFP could diffuse in all cells and that abscission remained incomplete in cyst expressing CycB5E.
(G) Fraction of egg chambers exhibiting more than 16 cells on the *y* axis. Genotypes are on the *x* axis. Expression of CycB-WT can partially suppress the CycB5E overexpression phenotype.
(H) Germarium expressing RNAi directed against *cycB* in germ cells (*nanos* driver), stained with DAPI (blue) and fusome (red). A stem cyst, formed of three cells, is shown (dotted line).
(I) *nos*>CycB-RNAi induces the formation of oocytes with five ring canals (arrows). F-actin stained with phalloidin.
(J) Germarium expressing *nos*>CycB-5E shows a fusome (green) breaking (arrow) in a two cell cyst (dotted line). α-spectrin (green).
(K) Germarium expressing *nos*>CycB-5E stained for EdU (red) and α-spectrin (green), showing that S-phase synchrony between the GSC (EdU-negative) and its CB (EdU-positive) is lost in these females.
(L) Fraction of GSC/CB pair showing S-phase asynchrony on the *y* axis in %. Genotypes are on the *x* axis.
(M) Fraction of egg chambers exhibiting less than 16 cells on the *y* axis. Genotypes are on the *x* axis. The loss of AurB can be rescued by expression of CycB5E only in the cyst with the *bam*-Gal4 driver.
(N) Example of a stage 7 "rescued" oocyte, mutant for aur^{B1689} and expressing *bam*>CycB-5E. Red arrows indicate the four ring canals in the oocyte.
Scale bar, 10 μm. See also Figure S4 and Movies S4, S5, and S6.

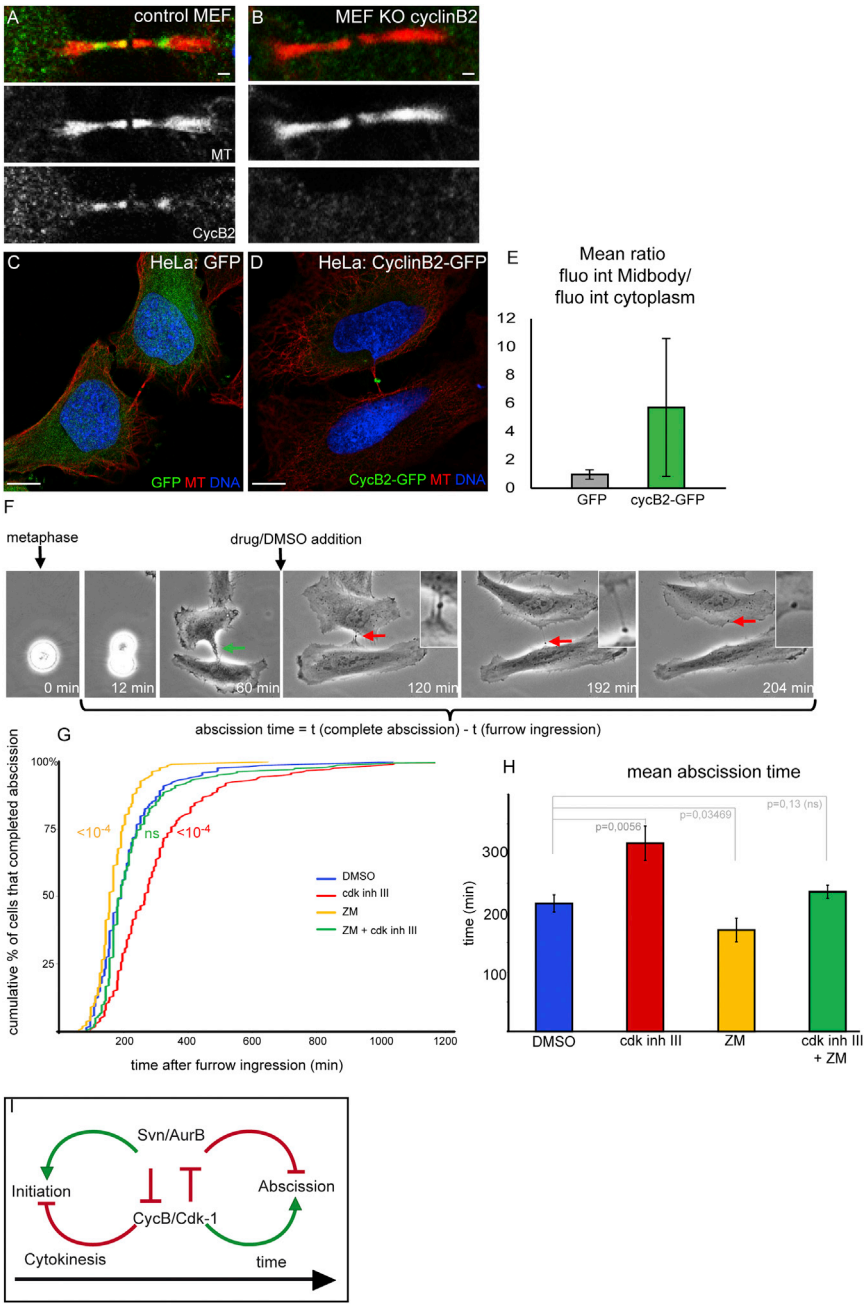

Figure 7. CycB2 Localizes at the Intercellular Bridge, and Cdk Activity Regulates Abscission Timing in Mammalian Cells

(A and B) Confocal sections of control (A) or Cyclin B2 knockout (B) MEFs stained for tubulin (red) and cyclin B2 (green).

(C and D) Confocal sections of HeLa cells transfected with GFP- (E) or Cyclin B2-GFP (F)-expressing vectors stained for tubulin (red) and DNA (DAPI; blue).

(E) Mean ratio of the fluorescence at the midbody/fluorescence in the cytoplasm of HeLa cells transfected with GFP (left, gray bar) or Cyclin B2-GFP (right, green bar). Error bars are SD.

(F) Cells were imaged from metaphase (time point [tp] 0 min) until abscission (tp 204 min). Drugs or DMSO were added only once furrow had ingressed into a thin bridge (green arrow, tp 60 min). Abscission duration was determined as the time between complete abscission and start of furrow ingression (tp 12 min). The midbody is visible as a dense structure in the bridge (see insets). At tp 204 min, the bridge is cut.

(G) Cumulative plot showing the fraction of HeLa cells (%) that have completed abscission in function of the duration of abscission (min) upon DMSO (n = 223), cdk1/2 inhibitor III (n = 215), ZM447439 (n = 223), or both drugs (n = 247). P values (Kolmogorov-Smirnov test) are indicated.

(H) Mean abscission duration of HeLa cells treated with cdk1/2 inhibitor III, ZM447439, or both drugs. P values (student test) are indicated. Error bars are SD.

(I) Schematic model of the interactions between the CPC and CycB/Cdk1 during early and late cytokinesis. See text for more details.

Scale bar, 10 μm. Error bars are SD.

in germline cysts and explain the eight-cell cysts, whereas inhibition of Cdk-1 could delay abscission in GSCs and produce 32-cell cysts. Furthermore, activation or inhibition of CycB/Cdk-1 in both GSC and cyst at the same time (as in homozygous mutants or overexpression using the *nanos* promoter) would lead to various combinations of opposite phenotypes (8, 16, and 32 cells), because loss or gain of function of CycB/Cdk-1 have opposite effects in the two cell types.

Inhibition of Abscission in Germline and Somatic Cells

One intriguing observation in our results is that a decrease of the CPC activity leads to the formation of cysts made of precisely eight cells, but not of four or two cells. It shows that the first division of the cystoblast is particularly sensitive to a reduction of Aurora B activity but not the three remaining divisions. In agreement, we only found breaking fusomes in two-cell cysts, but not in cysts with more branched fusomes. As described above, this phenotype is reminiscent of defects found in *bam* mutant ovaries (McKearin and Ohlstein, 1995). We thus propose that inhibition of abscission in the first division of the cystoblast is different from the three following mitosis. We suggest that initially this first division is very similar to a GSC division and both abscissions are delayed by Aurora B; however, when Bam starts to be expressed in cystoblasts, it triggers a developmental program, which completely blocks abscission of the first and following divisions, as previously proposed by McKearin and Ohlstein.

We believe that these findings have important implications for our understanding of abscission in germ cells but also in somatic cells in general. Cytokinesis can also be arrested in follicle cells and other somatic tissues where there is no fusome or transcription of *bam* (Airoldi et al., 2011; de Cuevas and

Spradling, 1998; Haglund et al., 2010). We further demonstrated that CycB2 localizes at the intercellular bridge and that Aurora B and Cdk-1 have opposite effects on abscission in vertebrate somatic cells. Interestingly, although mice knockout for Cyclin B2 are viable, males are less fertile and have small litter size (Brandeis et al., 1998). We speculate that germ cells may be more sensitive to abscission defects than somatic cells but that the underlying mechanisms are very similar.

EXPERIMENTAL PROCEDURES

Fly Strains

The *PBac2180* insertion was identified in a previous screen (Mathieu et al., 2007), and *PBac1527* was obtained at the Bloomington Stock Center. Mutations in *aurB* were generated during two independent EMS mutageneses and screens. The following alleles and transgenes were used: $bam^{\Delta 86}$ (Bopp et al., 1993); hts^{1}; hts^{01103} (Yue and Spradling, 1992); $cycB^{2}$ and $cycB^{3}$(Jacobs et al., 1998); $cycB^{KG08886}$ (Bloomington Stock Center); UAS-photoactivatable (PA)-GFP (Murray and Saint, 2007); *UAS-Trip cycB* (Ni et al., 2011); *Ubq-RFP-α-Tubulin* (Basto et al., 2008); *cid-RFP* (Schuh et al., 2007); *H2B-RFP* (Schuh et al., 2007); and *jupiter-GFP* (Karpova et al., 2006).

Cell Culture, Transfection, and Drug Treatments

Transfection of ATCC cells were performed using FuGENE-6 (Roche). The plasmid encoding myc-CycB2-GFP was obtained from J. Pines via J. Sobczack.

HEK293T (2.10^{6}) cells were transfected by the plasmids promoter cytomegalovirus (pCMV)-HA-AurB and/or pCMV-cycB-GFP (4 μg total) using polyethylenimine.

Cells have been treated with 2 μM ZM447439 (TOCRIS Bioscience) and/or with 300 nM cdk1/2 inhibitor III (Merck).

Constructs and Antibodies

To generate the genomic rescue construct of *survivin*, a PCR fragment corresponding to the *survivin* locus was amplified from genomic DNA. The making of *svn>svnΔBIR*, *svn>svnC97A*, *svn>svnS125A*, *svn>svnT129A*, *svn>svnS125A,T129A, UASp>svnWT-GFP, UASp>svn125E-GFP*, *tub>RFP-aurB*, *pUASp>RFP-aurA, pUASp>CycB-WT-GFP, pUASp>CycB-5A-GFP*, and *pUASp>CycB-5E-GFP* are detailed in the Supplemental Experimental Procedures.

A phosphorylated Cyclin B peptide, $SNLSKKS_{157}$(PO3H2)LTKLR, corresponding to the fourth potential Aurora-B phosphorylation site, was synthesized and used for immunization of two rabbits (Eurogentec).

Quantification and Statistics

We counted the number of nuclei with the DAPI staining. In addition, the number of ring canals stained by phalloidin was counted for the oocyte to discard encapsulation defects. Chi-square tests were used to compare the proportions of egg chambers having 8, 16, or 32 cells.

Microscopy

Acquisition of Z stacks on fixed sample was carried out on Zeiss LSM710 or LSM780 confocal microscopes. For live imaging of germarium, ovaries were dissected and mounted in oil and were imaged with an inverted Confocal Spinning Disk Roper/Nikon.

HeLa cells were plated on 35 mm glass dishes, and time-lapse sequences were recorded every 10 or 12 min for 24 hr on a Nikon Eclipse Ti microscope with a 20X 0.45 numerical aperture Plan Fluor Extra Long Working Distances objective lens controlled by Metamorph 6.1 software (Universal Imaging).

Photoactivation was done with a two-photon laser at 820 nm. Imaging was done with a Zeiss LSM 710.

SUPPLEMENTAL INFORMATION

Supplemental Information includes Supplemental Experimental Procedures, seven figures, and seven movies and can be found with this article online at http://dx.doi.org/10.1016/j.devcel.2013.07.005.

ACKNOWLEDGMENTS

We are grateful to M. Bettencourt-Dias, S. Campbell, M. Carmena, M. Carrington, O. Gavet, D. Glover, B. Earnshaw, I. Ferreira, M. Gho, J. Raff, S. Ruchaud, J. Sobszack, and P. ten Dijke for helpful discussions, advice, and materials. We thank members of the Huynh laboratory, A. Gonzalez-Reyes, and E. Heard for critical reading of the manuscript, DSHB (Iowa University) for antibodies, and the Bloomington Drosophila Stock Center for fly stocks. We thank the imaging facility (PICT@BDD) and the proteomic platform for excellent technical help. This work was supported by the CNRS, ANR (ANR-06-JCJC-0092), ARC postdoctoral fellowship (to J.M.), FSER (Schlumberger), Ville de Paris, and Fondation BNP-Paribas (to J.-R.H.). A.E. was supported by CNRS, Institut Pasteur, équipe FRM2012 and FSER (Schlumberger).

Received: February 16, 2013
Revised: April 10, 2013
Accepted: July 9, 2013
Published: August 12, 2013

REFERENCES

Adams, R.R., Maiato, H., Earnshaw, W.C., and Carmena, M. (2001). Essential roles of Drosophila inner centromere protein (INCENP) and aurora B in histone H3 phosphorylation, metaphase chromosome alignment, kinetochore disjunction, and chromosome segregation. J. Cell Biol. *153*, 865–880.

Airoldi, S.J., McLean, P.F., Shimada, Y., and Cooley, L. (2011). Intercellular protein movement in syncytial Drosophila follicle cells. J. Cell Sci. *124*, 4077–4086.

Basto, R., Brunk, K., Vinadogrova, T., Peel, N., Franz, A., Khodjakov, A., and Raff, J.W. (2008). Centrosome amplification can initiate tumorigenesis in flies. Cell *133*, 1032–1042.

Bopp, D., Horabin, J.I., Lersch, R.A., Cline, T.W., and Schedl, P. (1993). Expression of the Sex-lethal gene is controlled at multiple levels during Drosophila oogenesis. Development *118*, 797–812.

Brandeis, M., Rosewell, I., Carrington, M., Crompton, T., Jacobs, M.A., Kirk, J., Gannon, J., and Hunt, T. (1998). Cyclin B2-null mice develop normally and are fertile whereas cyclin B1-null mice die in utero. Proc. Natl. Acad. Sci. USA *95*, 4344–4349.

Burkard, M.E., Randall, C.L., Larochelle, S., Zhang, C., Shokat, K.M., Fisher, R.P., and Jallepalli, P.V. (2007). Chemical genetics reveals the requirement for Polo-like kinase 1 activity in positioning RhoA and triggering cytokinesis in human cells. Proc. Natl. Acad. Sci. USA *104*, 4383–4388.

Chen, S., Wang, S., and Xie, T. (2011). Restricting self-renewal signals within the stem cell niche: multiple levels of control. Curr. Opin. Genet. Dev. *21*, 684–689.

Clute, P., and Pines, J. (1999). Temporal and spatial control of cyclin B1 destruction in metaphase. Nat. Cell Biol. *1*, 82–87.

de Cuevas, M., and Spradling, A.C. (1998). Morphogenesis of the Drosophila fusome and its implications for oocyte specification. Development *125*, 2781–2789.

Echard, A., and O'Farrell, P.H. (2003). The degradation of two mitotic cyclins contributes to the timing of cytokinesis. Curr. Biol. *13*, 373–383.

Eluère, R., Offner, N., Varlet, I., Motteux, O., Signon, L., Picard, A., Bailly, E., and Simon, M.N. (2007). Compartmentalization of the functions and regulation of the mitotic cyclin Clb2 in S. cerevisiae. J. Cell Sci. *120*, 702–711.

Gavet, O., and Pines, J. (2010a). Activation of cyclin B1-Cdk1 synchronizes events in the nucleus and the cytoplasm at mitosis. J. Cell Biol. *189*, 247–259.

Gavet, O., and Pines, J. (2010b). Progressive activation of CyclinB1-Cdk1 coordinates entry to mitosis. Dev. Cell *18*, 533–543.

Gilboa, L., and Lehmann, R. (2004). Repression of primordial germ cell differentiation parallels germ line stem cell maintenance. Curr. Biol. *14*, 981–986.

Gilboa, L., Forbes, A., Tazuke, S.I., Fuller, M.T., and Lehmann, R. (2003). Germ line stem cell differentiation in Drosophila requires gap junctions and proceeds via an intermediate state. Development *130*, 6625–6634.

Gruneberg, U., Neef, R., Honda, R., Nigg, E.A., and Barr, F.A. (2004). Relocation of Aurora B from centromeres to the central spindle at the metaphase to anaphase transition requires MKlp2. J. Cell Biol. *166*, 167–172.

Haglund, K., Nezis, I.P., Lemus, D., Grabbe, C., Wesche, J., Liestøl, K., Dikic, I., Palmer, R., and Stenmark, H. (2010). Cindr interacts with anillin to control cytokinesis in Drosophila melanogaster. Curr. Biol. *20*, 944–950.

Hümmer, S., and Mayer, T.U. (2009). Cdk1 negatively regulates midzone localization of the mitotic kinesin Mklp2 and the chromosomal passenger complex. Curr. Biol. *19*, 607–612.

Huynh, J.R. (2005). Fusome as a cell-cell communication channel of *Drosophila* ovarian cyst. In Cell-Cell Channels, F. Baluska, D. Volkmann, and P.W. Barlow, eds. (Georgetown, TX: Landes Biosciences).

Huynh, J.R., and St Johnston, D. (2004). The origin of asymmetry: early polarisation of the Drosophila germline cyst and oocyte. Curr. Biol. *14*, R438–R449.

Jacobs, H.W., Knoblich, J.A., and Lehner, C.F. (1998). Drosophila Cyclin B3 is required for female fertility and is dispensable for mitosis like Cyclin B. Genes Dev. *12*, 3741–3751.

Jin, Z., Homola, E.M., Goldbach, P., Choi, Y., Brill, J.A., and Campbell, S.D. (2005). Drosophila Myt1 is a Cdk1 inhibitory kinase that regulates multiple aspects of cell cycle behavior during gametogenesis. Development *132*, 4075–4085.

Jones, G., Jones, D., Zhou, L., Steller, H., and Chu, Y. (2000). Deterin, a new inhibitor of apoptosis from Drosophila melanogaster. J. Biol. Chem. *275*, 22157–22165.

Kai, T., and Spradling, A. (2004). Differentiating germ cells can revert into functional stem cells in Drosophila melanogaster ovaries. Nature *428*, 564–569.

Karpova, N., Bobinnec, Y., Fouix, S., Huitorel, P., and Debec, A. (2006). Jupiter, a new Drosophila protein associated with microtubules. Cell Motil. Cytoskeleton *63*, 301–312.

Lens, S.M., Rodriguez, J.A., Vader, G., Span, S.W., Giaccone, G., and Medema, R.H. (2006). Uncoupling the central spindle-associated function of the chromosomal passenger complex from its role at centromeres. Mol. Biol. Cell *17*, 1897–1909.

Lilly, M.A., and Spradling, A.C. (1996). The Drosophila endocycle is controlled by Cyclin E and lacks a checkpoint ensuring S-phase completion. Genes Dev. *10*, 2514–2526.

Lilly, M.A., de Cuevas, M., and Spradling, A.C. (2000). Cyclin A associates with the fusome during germline cyst formation in the Drosophila ovary. Dev. Biol. *218*, 53–63.

Lindqvist, A., Rodríguez-Bravo, V., and Medema, R.H. (2009). The decision to enter mitosis: feedback and redundancy in the mitotic entry network. J. Cell Biol. *185*, 193–202.

Malumbres, M., and Barbacid, M. (2009). Cell cycle, CDKs and cancer: a changing paradigm. Nat. Rev. Cancer *9*, 153–166.

Mata, J., Curado, S., Ephrussi, A., and Rørth, P. (2000). Tribbles coordinates mitosis and morphogenesis in Drosophila by regulating string/CDC25 proteolysis. Cell *101*, 511–522.

Mathieu, J., Sung, H.H., Pugieux, C., Soetaert, J., and Rorth, P. (2007). A sensitized PiggyBac-based screen for regulators of border cell migration in Drosophila. Genetics *176*, 1579–1590.

McKearin, D., and Ohlstein, B. (1995). A role for the Drosophila bag-of-marbles protein in the differentiation of cystoblasts from germline stem cells. Development *121*, 2937–2947.

Morris, L.X., and Spradling, A.C. (2011). Long-term live imaging provides new insight into stem cell regulation and germline-soma coordination in the Drosophila ovary. Development *138*, 2207–2215.

Murray, M.J., and Saint, R. (2007). Photoactivatable GFP resolves Drosophila mesoderm migration behaviour. Development *134*, 3975–3983.

Neef, R., Preisinger, C., Sutcliffe, J., Kopajtich, R., Nigg, E.A., Mayer, T.U., and Barr, F.A. (2003). Phosphorylation of mitotic kinesin-like protein 2 by polo-like kinase 1 is required for cytokinesis. J. Cell Biol. *162*, 863–875.

Ni, J.Q., Zhou, R., Czech, B., Liu, L.P., Holderbaum, L., Yang-Zhou, D., Shim, H.S., Tao, R., Handler, D., Karpowicz, P., et al. (2011). A genome-scale shRNA resource for transgenic RNAi in Drosophila. Nat. Methods *8*, 405–407.

Norden, C., Mendoza, M., Dobbelaere, J., Kotwaliwale, C.V., Biggins, S., and Barral, Y. (2006). The NoCut pathway links completion of cytokinesis to spindle midzone function to prevent chromosome breakage. Cell *125*, 85–98.

Ohlmeyer, J.T., and Schüpbach, T. (2003). Encore facilitates SCF-Ubiquitin-proteasome-dependent proteolysis during Drosophila oogenesis. Development *130*, 6339–6349.

Parry, D.H., Hickson, G.R., and O'Farrell, P.H. (2003). Cyclin B destruction triggers changes in kinetochore behavior essential for successful anaphase. Curr. Biol. *13*, 647–653.

Pepling, M.E., de Cuevas, M., and Spradling, A.C. (1999). Germline cysts: a conserved phase of germ cell development? Trends Cell Biol. *9*, 257–262.

Petronczki, M., Glotzer, M., Kraut, N., and Peters, J.M. (2007). Polo-like kinase 1 triggers the initiation of cytokinesis in human cells by promoting recruitment of the RhoGEF Ect2 to the central spindle. Dev. Cell *12*, 713–725.

Pines, J. (2006). Mitosis: a matter of getting rid of the right protein at the right time. Trends Cell Biol. *16*, 55–63.

Ruchaud, S., Carmena, M., and Earnshaw, W.C. (2007). Chromosomal passengers: conducting cell division. Nat. Rev. Mol. Cell Biol. *8*, 798–812.

Sanger, J.M., Pochapin, M.B., and Sanger, J.W. (1985). Midbody sealing after cytokinesis in embryos of the sea urchin Arabacia punctulata. Cell Tissue Res. *240*, 287–292.

Schuh, M., Lehner, C.F., and Heidmann, S. (2007). Incorporation of Drosophila CID/CENP-A and CENP-C into centromeres during early embryonic anaphase. Curr. Biol. *17*, 237–243.

Sigrist, S., Jacobs, H., Stratmann, R., and Lehner, C.F. (1995). Exit from mitosis is regulated by Drosophila fizzy and the sequential destruction of cyclins A, B and B3. EMBO J. *14*, 4827–4838.

Skop, A.R., Liu, H., Yates, J., 3rd, Meyer, B.J., and Heald, R. (2004). Dissection of the mammalian midbody proteome reveals conserved cytokinesis mechanisms. Science *305*, 61–66.

Snapp, E.L., Iida, T., Frescas, D., Lippincott-Schwartz, J., and Lilly, M.A. (2004). The fusome mediates intercellular endoplasmic reticulum connectivity in Drosophila ovarian cysts. Mol. Biol. Cell *15*, 4512–4521.

Song, X., Wong, M.D., Kawase, E., Xi, R., Ding, B.C., McCarthy, J.J., and Xie, T. (2004). Bmp signals from niche cells directly repress transcription of a differentiation-promoting gene, bag of marbles, in germline stem cells in the Drosophila ovary. Development *131*, 1353–1364.

Spradling, A. (1993a). Developmental genetics of oogenesis. In The Development of *Drosophila melanogaster*, M. Bate and A. Martinez-Arias, eds. (New York: Cold Spring Harbor Laboratory Press), pp. 1–70.

Spradling, A.C. (1993b). Germline cysts: communes that work. Cell *72*, 649–651.

Steigemann, P., Wurzenberger, C., Schmitz, M.H., Held, M., Guizetti, J., Maar, S., and Gerlich, D.W. (2009). Aurora B-mediated abscission checkpoint protects against tetraploidization. Cell *136*, 473–484.

Sullivan, M., and Morgan, D.O. (2007). Finishing mitosis, one step at a time. Nat. Rev. Mol. Cell Biol. *8*, 894–903.

Terada, Y., Tatsuka, M., Suzuki, F., Yasuda, Y., Fujita, S., and Otsu, M. (1998). AIM-1: a mammalian midbody-associated protein required for cytokinesis. EMBO J. *17*, 667–676.

Tsukahara, T., Tanno, Y., and Watanabe, Y. (2010). Phosphorylation of the CPC by Cdk1 promotes chromosome bi-orientation. Nature *467*, 719–723.

Vitrat, N., Cohen-Solal, K., Pique, C., Le Couedic, J.P., Norol, F., Larsen, A.K., Katz, A., Vainchenker, W., and Debili, N. (1998). Endomitosis of human megakaryocytes are due to abortive mitosis. Blood *91*, 3711–3723.

Wang, Z., and Lin, H. (2005). The division of Drosophila germline stem cells and their precursors requires a specific cyclin. Curr. Biol. *15*, 328–333.

Wheatley, S.P., Henzing, A.J., Dodson, H., Khaled, W., and Earnshaw, W.C. (2004). Aurora-B phosphorylation in vitro identifies a residue of survivin that is essential for its localization and binding to inner centromere protein (INCENP) in vivo. J. Biol. Chem. *279*, 5655–5660.

Wurzenberger, C., and Gerlich, D.W. (2011). Phosphatases: providing safe passage through mitotic exit. Nat. Rev. Mol. Cell Biol. *12*, 469–482.

Yue, L., and Spradling, A.C. (1992). hu-li tai shao, a gene required for ring canal formation during Drosophila oogenesis, encodes a homolog of adducin. Genes Dev. *6*(12B), 2443–2454.

Yue, Z., Carvalho, A., Xu, Z., Yuan, X., Cardinale, S., Ribeiro, S., Lai, F., Ogawa, H., Gudmundsdottir, E., Gassmann, R., et al. (2008). Deconstructing Survivin: comprehensive genetic analysis of Survivin function by conditional knockout in a vertebrate cell line. J. Cell Biol. *183*, 279–296.